Dynamic and Performance Modeling of Multistage Manufacturing Systems using Nonlinear Stochastic Differential Equation (1)

Utkarsh Mittal[1]

[1]Affiliation not available

December 10, 2023

4th IEEE Conference on Automation Science and Engineering
Key Bridge Marriott, Washington DC, USA
August 23-26, 2008

Dynamics and Performance Modeling of Multi-Stage Manufacturing Systems using Nonlinear Stochastic Differential Equations

Utkarsh Mittal[1], Hui Yang[1*], Satish T.S. Bukkapatnam[1], and Leandro G. Barajas[2]

Abstract — Modern manufacturing enterprises have invested in a variety of sensors and IT infrastructure to increase plant floor information visibility. This offers an unprecedented opportunity to track performances of manufacturing systems from a dynamic, as opposed to static, sense. Conventional static models are inadequate to model manufacturing system performance variations in real-time from these large non-stationary data sources. This paper addresses a physics-based approach to model the performance outputs (e.g., throughputs, uptimes, and yield rates) from a multi-stage manufacturing system. Unlike previous methods, degradation and repair dynamics that influence downtime distributions in such manufacturing systems are explicitly considered. Sigmoid function theory is used to remove discontinuities in the models. The resulting model is validated using real-world datasets acquired from the General Motor's assembly lines, and it is found to capture dynamics of downtime better than traditional exponential distribution based simulation models.

Index Terms — **nonlinear stochastic differential equation (n-SDE) model, mean time between failure (MTBF), mean time to repair (MTTR), recurrence analysis, multi-stage manufacturing systems**

I. Introduction

Increasing global competition is forcing many automotive, aerospace and microelectronic manufacturing systems towards low margins and lean operations. More than ever, customers are demanding lower prices, short turnaround times, higher quality, and customized designs. In order to stay competitive under volatile demands as well as internal and external disruptions, modern manufacturing systems need to dynamically adjust product mix, plan near-term capacity, and manage suppliers and dealers with little time latency.

Accurate real-time prediction of performance is essential for making a manufacturing system respond in a fast and flexible manner to demand variations and disruptions. Performance of manufacturing systems, such as automotive manufacturing lines, are typically expressed in terms of throughput rates, throughput losses due to breakdowns, blocking and starving, and WIP levels [1].

However, conventional static models are inadequate for predicting these performance variables in real-time, therefore, dynamic models are necessary. Modern manufacturing systems are pervasively networked to carefully monitor and record most events and statuses, e.g., start and end of operations, fault events, exceptions and errors, etc. Hundreds of messages related to performance variables can be generated in every second. Dynamic models can compactly capture information from these real-time data sources and thus help track the performances of a manufacturing system from a dynamic, as opposed to conventional static, sense.

Recent advancements on sensing techniques and computing power have compelled the research community to show a renewed interest in continuous flow modeling approaches [2-7]. Continuous flow modeling approaches can offer an effective balance between accuracy and speed. These approaches essentially model the parts movement in a manufacturing system as a fluid flow expressed in the form of differential equations. This is a reasonable assumption that enable us to capture dynamics of several manufacturing systems including automotive and semiconductor production lines where part inter-release time-scales are much shorter than those for other perturbation events. These models offer several advantages including faster simulations and enhanced identification of the system dynamic patterns compared to discrete-event simulations (DES). While queuing network models and micro DES have received significant attention, aggregate modeling has received little attention in the domain of manufacturing systems. Many of the recent pioneering works have applied these models to gain certain crucial qualitative insights into the plant-floor and into the enterprise-level system characteristics [2-12]. Few works have shown the potential of time-aggregated flow models for performance monitoring and prediction.

We present an approach that uses the sigmoid function theory to relax certain assumptions made on the instantaneous nature of up and down time events. The resulting simulation model is found to capture the dynamics of downtime better than conventional exponential distribution based simulation models. The remainder of this paper is organized as follows: Section II presents a physics-

Manuscript received June 27, 2008.

[1]Utkarsh Mittal, Hui Yang* and Satish T.S. Bukkapatnam are with School of Industrial Engineering and Management, Oklahoma State University, Stillwater, OK 74075 USA (e-mail: Utkarsh@okstate.edu, hui.yang@okstate.edu, satish.t.bukkapatnam@okstate.edu).

[2]Leadro Barajas is with the Manufacturing Systems Research Laboratory in General Motor R&D Center, Warren, MI, 48090 (e-mail: leandro.barajas@gm.com).

based nonlinear stochastic differential equation (n-SDE) modeling approach; Section III demonstrates the n-SDE model parameterization using a genetic algorithm, comparisons of the resulting probability density functions (PDF) of the n-SDE and Exponential models versus the actual realizations, and nonlinear dynamic quantification of the investigated models versus the actual field data. Finally, Section IV presents the conclusions of the reported research and perspectives on future investigations.

II. Physics Based N-SDE Modeling Approach

Physics-based models use the first-principle physical and logical relationships in manufacturing systems to derive functional forms, and the aggregated line statistics to parameterize the models (just as how one derives DES models). For a simple N-stage manufacturing system, the change in the length of the buffer at the downstream of the k^{th} operation is given by

$$dL_k/dt = u_{k-1} - u_k \tag{1}$$

where u_k is the throughput velocity of operation k, L_k is the buffer inventory level. Typically, u_k is modeled using random processes μ_k and ν_k as

$$u_k = \mu_k - \nu_k \tag{2}$$

where μ_k is the processing rate during uptime, ν_k is the throughput rate loss due to downtime (alternative treatments of machine breakdown as a valve or a switch have been considered) , and $u_k = 0$ during downtime [13]. Downtime in many manufacturing system operations (see Fig. 1) can occur due to the following three reasons: (1) Machine breakdown and repair that takes place during times $t \in \mathbb{T}_{repair}$, (2) Starving (upstream buffer is empty) that takes place during times $t \in \mathbb{T}_{starve}$ and/or (3)Blocking (downstream buffer is full) that takes place during times $t \in \mathbb{T}_{block}$, i.e.,

$$u_k = 0 \text{ if } (L_k \le 0,\ L_{k+1} > L^{max}_{k+1},\ t \in \mathbb{T}_{\text{repair}}) \tag{3}$$

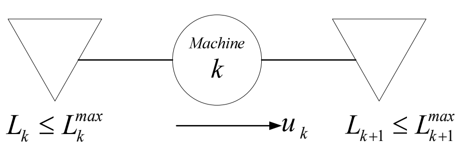

Fig. 1 *Blocking and starving operation in an assembly line*

The aforementioned flow modeling approaches have traditionally been used for qualitative analysis of system dynamics and not for real-time performance estimation. However, discontinuities in flow adversely affect the integration routines used to solve the model, and often cause the routines to become unstable. Sigmoid function theory is applied to derive equivalent analytic forms of the vector flow fields, whose integration methods pose less numerical instability issues and is expected to enable much faster simulation of system dynamics.

As shown in Fig. 2, the operation downtime due to machine breakdown and repair is simulated from a dynamic interplay between the machine degradation condition β and the restoration effort ρ. Intuitively, the machine will breakdown if the machine condition drops below a threshold β^0. At this point the restoration process which proceeds from its base level ρ^- will start. As the restoration efforts (including diagnostics) proceed, the machine condition steadily bottoms out, improves from its lowest level β^- and above to a full restoration level β^+. About this point, the restoration efforts are relaxed out.

Such a dynamic interplay can be effectively captured using coupled nonlinear stochastic differential equations (n-SDEs) [6, 7]. For example, the machine degradation dynamics can be captured using a first order nonlinear differential equation of the form

$$\begin{aligned}\frac{d\beta}{dt} = {} & K_1 \cdot \mathrm{sgm}\big(w_1(a_1-\beta)\big)\mathrm{sgm}\big(-w_2(\rho-a_2)\big) \\ & + K_2 \cdot \mathrm{sgm}\big(w_3(\rho-a_3)\big)\mathrm{sgm}\big(w_4(\beta-a_4)\big)\end{aligned} \tag{4}$$

and the restoration (damage-repair) dynamics is captured using the following second order differential equation

$$\begin{aligned}\frac{d^2\rho}{dt^2} = {} & K_3 \cdot \mathrm{sgm}\big(w_5(\dot{\rho}-a_5)\big)\mathrm{sgm}\big(w_6(\beta-a_6)\big) \\ & + K_4 \cdot \mathrm{sgm}\big(w_7(a_7-\beta)\big)\mathrm{sgm}\big(w_8(a_8-\dot{\rho})\big)\end{aligned} \tag{5}$$

where a_{1-8} and w_{1-8} are the threshold values and K_{1-4} and the weights of sigmoid functions of the form

$$\mathrm{sgm}\big(w_j(\beta-a_j)\big) = \left(1+e^{-w_j(\beta-a_j)}\right)^{-1} \tag{6}$$

which are the structural parameters of the model. Evidently, such sigmoid functions can be used to adjust throughput rate for each operation for downtime as well as for starve/block conditions as

$$u_k = \mu_k sgm(L_k) sgm(L^{max}_{k+1} - L_{k+1}) sgm(\beta_k - \beta^0_k)\,. \tag{7}$$

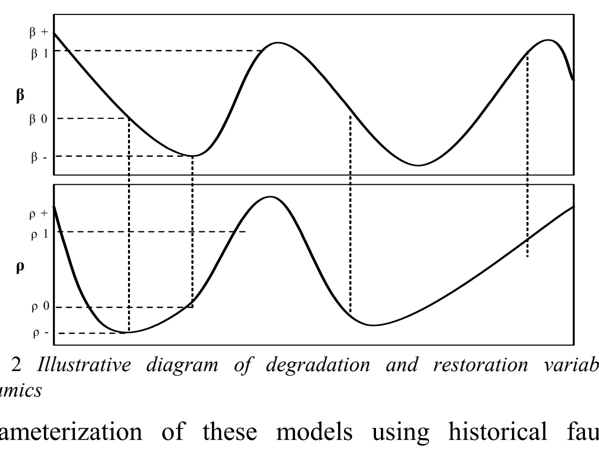

Fig. 2 *Illustrative diagram of degradation and restoration variable dynamics*

Parameterization of these models using historical fault distributions, such as distributions of time between failure (TBF) and time to repair (TTR), can be significantly challenging. We used a genetic algorithm for parameterization. The following fitness function *Op* defined in Eq. 8 is based on the empirical distributions of TTR and TBF obtained through histogram transformation of actual data and the model outputs:

$$
\begin{aligned}
Op = {} & 100\left(\frac{\sum_{k=1}^{N_0}(HistTBF(k)-HistTBFa(k))^2}{N_0}+\frac{\sum_{k=1}^{N_1}(HistTTR(k)-HistTTRa(k))^2}{N_1}\right)+ \\
& 10\left(\frac{\sum_{k=N_0+1}^{N_0+N_2}(HistTBF(k)-HistTBFa(k))^2}{N_2}+\frac{\sum_{k=N_1+1}^{N_1+N_3}(HistTTR(k)-HistTTRa(k))^2}{N_3}\right)+ \\
& \left(\frac{\sum_{k=N_0+N_2+1}^{N_0+N_2+N_4}(HistTBF(k)-HistTBFa(k))^2}{N_4}+\frac{\sum_{k=N_1+N_3+1}^{N_1+N_3+N_5}(HistTTR(k)-HistTTRa(k))^2}{N_5}\right)
\end{aligned}
\quad (8)
$$

where k is the bin index. The histograms of TBF from the model (*HistTBF*) and the actual data (*HistTBFa*) are divided into three areas: N_0, N_2, N_4 are the number of bins used for the three areas to compare histogram transformations of TBF distribution from the model (*HistTBF*) with that from actual data (*HistTBFa*). Similarly, N_1, N_3, N_5 are the corresponding bins used to compare histogram transformations of TTR distribution from the model (*HistTTR*) with actual historic data (*HistTTRa*). The weights for the three areas of the histogram are assigned to be 100, 10, 1 that signify their relative importance from an operational standpoint. For instance, the values in the histogram bins with a weight of 100 are considered to be in the normal range of TBF/TTR, while the bins with smaller weights are taken to capture the highly infrequent instances of TBF/TTR where the number of samples is few. We parameterized the n-SDE models for each of the 18 machines in a real-world assembly line segment. The line segment considered for the present investigation consists of 18 stations of which 17 are allocated in tandem. One pair of stations is located in a parallel arrangement in the assembly line. We used the actual occurrences of various faults to derive distributions for TBF and TTR. The simulated as well as the actual TBF and TTR data were gathered over a two-month long period.

III. N-SDE Model Parameterization and Results

The Genetic Algorithm (GA) aims to determine the optimal values for 17 n-SDE model parameters namely a_1, a_2, a_3, a_4, a_5, a_6, a_{71}, a_{72}, a_8, k_{11}, k_{12}, k_{21}, k_{22}, k_{31}, k_{32}, k_{41}, k_{42} that reduce Op values to below 10^{-2}, such that TTR and TBF distributions closely match with those derived from the actual data. The GA procedure begins with the generation of the initial set of 50 different combinations of parameter vector values that are random within the allowable range for the 17 parameters n-SDE model. Each parameter was encoded as 35-bit long binary string. The objective function Op corresponding to this generated set of parameters is evaluated. Standard genetic operators like roulette-wheel selection, crossover, and mutation are used to generate a new set of 20 coded parameter values and the fitness function is then reevaluated. The GA terminates after the maximum number of iterations are reached or when the Genetic Algorithm converges.

For the cases examined, GA is found to converge in less than 50 iterations. To refine the fitness of the solutions a Nelder-Mead simplex method is used. Once the fitness improvement rate drops below a threshold level, it is assumed that the parameter values lie in the basin of the global minimum because non-gradient based stochastic GA optimization methods are known to locate the basin (trough/crest) of the global optimum with a very high probability.

The resulting GA-parameterized model can capture the dynamics of machine degradation as well as the distributions of downtime, especially the time between failures (TBF) and time to repair (TTR) better than conventional exponential distribution models. For instance, Fig.3 shows the marginal PDFs of TTR for an operation at a assembly station obtained from the actual historical data (solid blue line) vs. the distribution obtained from the model (red dash line) vs. the one obtained using the best fit exponential distribution (green dash dotted line).

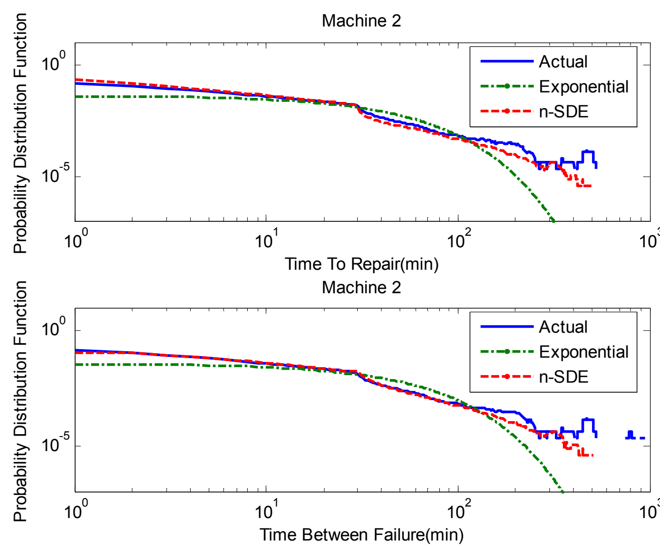

Fig. 3 *Comparison of marginal PDFs of TTR and TBF obtained from actual data (blue), n-SDE model (red) and exponential distribution model (green)*

Table 1 compares the mean, standard deviation, % deviation between model for TTR and TBF for machine 2. Moreover, the investigated model shows a mean square error which is one order in magnitude smaller than the one from the exponential model.

TABLE 1. COMPARISON OF MEAN, STANDARD DEVIATION, % DEVIATION OF MEAN AND STANDARD DEVIATION FOR MACHINE 2 TTR AND TBF

Mean TTR		**Std Dev TTR**		**Mean TBF**		**Std Dev TBF**	
Actual	Model	Actual	Model	Actual	Model	Actual	Model
9.41	9.24	13.59	15.11	27.35	24.71	29.42	25.28
% dev.		% dev		% dev		% dev	
1.81		10.1%		9.67%		14.05%	

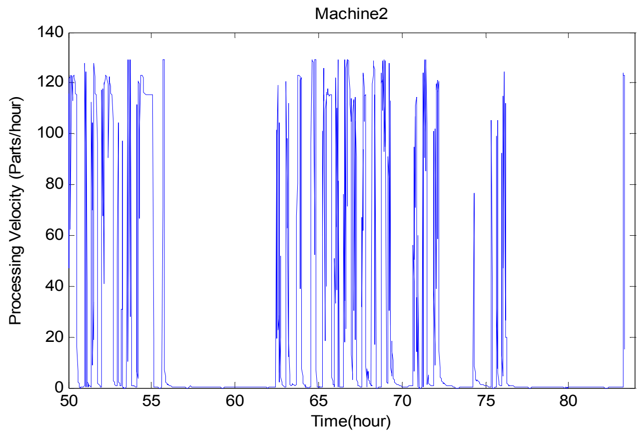

Fig. 4 *Processing Velocity for Machine 2*

Fig. 4 shows the variations of processing velocity with time for Machine 2. Maximum processing velocity for Machine 2 obtained from the actual data is 129 jobs/hour. This value is likely to occur, as is evident from Eq. (7), whenever the upstream buffer is full and the downstream buffer is empty and the machine is up. Also evident from the examining the histogram of the processing velocities (Fig. 5) is that the machine is down for longer duration than when it is operating at the peak velocity.

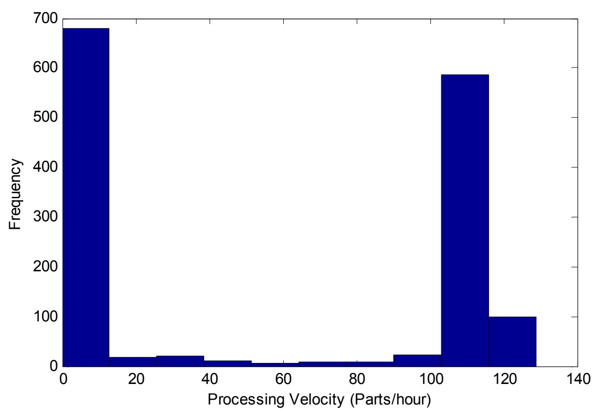

Fig. 5 *Histogram for Processing Velocity for Machine 2*

Table 2 shows the comparison between the processing velocity, expressed in terms of jobs per hour, from actual data versus the model. The average jobs/hour (processing velocity) from the actual and the model are 37.29 jobs/hour and 39.50 jobs/hour, respectively. The deviation between the model and the actual is 5.59%, which makes it quite comparable.

TABLE 2. COMPARISON OF PROCESSING VELOCITY BETWEEN MODEL AND ACTUAL

Jobs/Hour		**%Deviation Jobs/Hour**
Actual	Model	5.59 %
37.20	39.50	

Fig. 6 and Fig.7 compare the mean time to repair (MTTR) and mean time between failure (MTBF) for the 18 machines from the model vs. the actual data. The actual statistics are shown in brown bars and the model outputs are shown in blue. The comparisons show that the proposed model can capture the MTTR and MTBF variations from machine to machine for the investigated assembly line segment. The result shows that MTBF computed from the model lies within 3-10% of that computed from the actual data for 10 out of 18 machines. The model-computed MTBF values for the remaining 8 machines vary on an average by 24% relative to those computed from actual data. Similarly, the model-computed TTR values for 10 machines vary between 2-8% of those computed from the actual data, and vary by an average of 28% from those computed from the actual data for the remaining 8 machines.

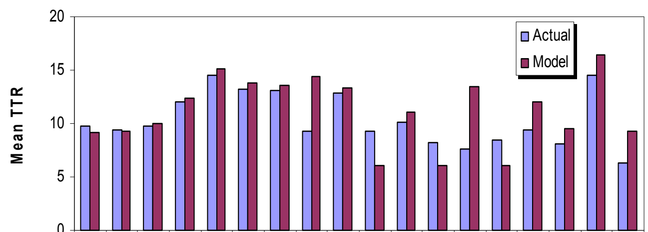

	1	2	3	4	5	6	7	8	9	10	12	13A	13B	14	15	16	17	18
Actual	9.82	9.42	9.79	12	14.5	13.2	13.1	9.34	12.9	9.23	10.2	8.21	7.56	8.47	9.4	8.04	14.5	6.26
Model	9.15	9.25	9.99	12.4	15.2	13.8	13.5	14.4	13.3	6.05	11.1	6.05	13.5	6.05	12.1	9.56	16.4	9.29

Fig. 6 *Comparison of Mean TTR (Model vs. Actual)*

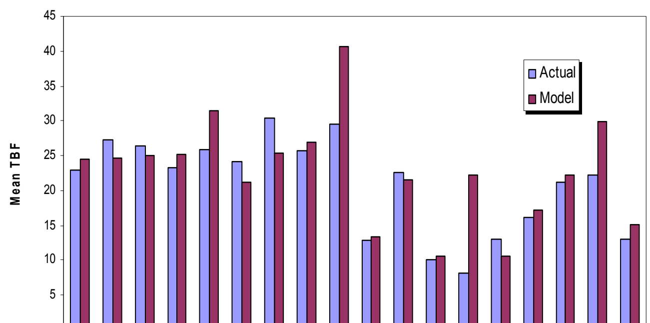

	1	2	3	4	5	6	7	8	9	10	12	13A	13B	14	15	16	17	18
Actual	22.95	27.36	26.46	23.29	25.84	24.09	30.33	25.78	29.56	12.89	22.52	10.16	8.183	13.06	16.15	21.23	22.23	12.99
Model	24.42	24.71	25.05	25.16	31.48	21.22	25.31	27.01	40.74	13.31	21.62	10.58	22.25	10.58	17.19	22.26	29.97	15.04

Fig. 7 *Comparison of Mean TBF (Model vs. Actual)*

Traditional simulation models use the distributions for TTR and TBF that capture the static characteristic, but not the dynamics. In this investigation, nonlinear dynamics characterization methods, for e.g., recurrence quantification analysis, are used to extract quantifiers for deciding the dimension of the state vector and functional forms of vector fields of n-SDE models. Recurrence methods capture the topological relationships (including several nonlinear dynamics and non-stationarity related manifestations) existing in this state-space as a 2-dimensional representation. Fig. 8 shows representative unthresholded (top) and thresholded (bottom) recurrence plots of TBF and TTR for n-SDE, actual and exponential models from an assembly line segment. Recurrence plots from n-SDE and actual model show complex (nonlinear) and irregular (stochastic) texture patterns while the one from exponential model

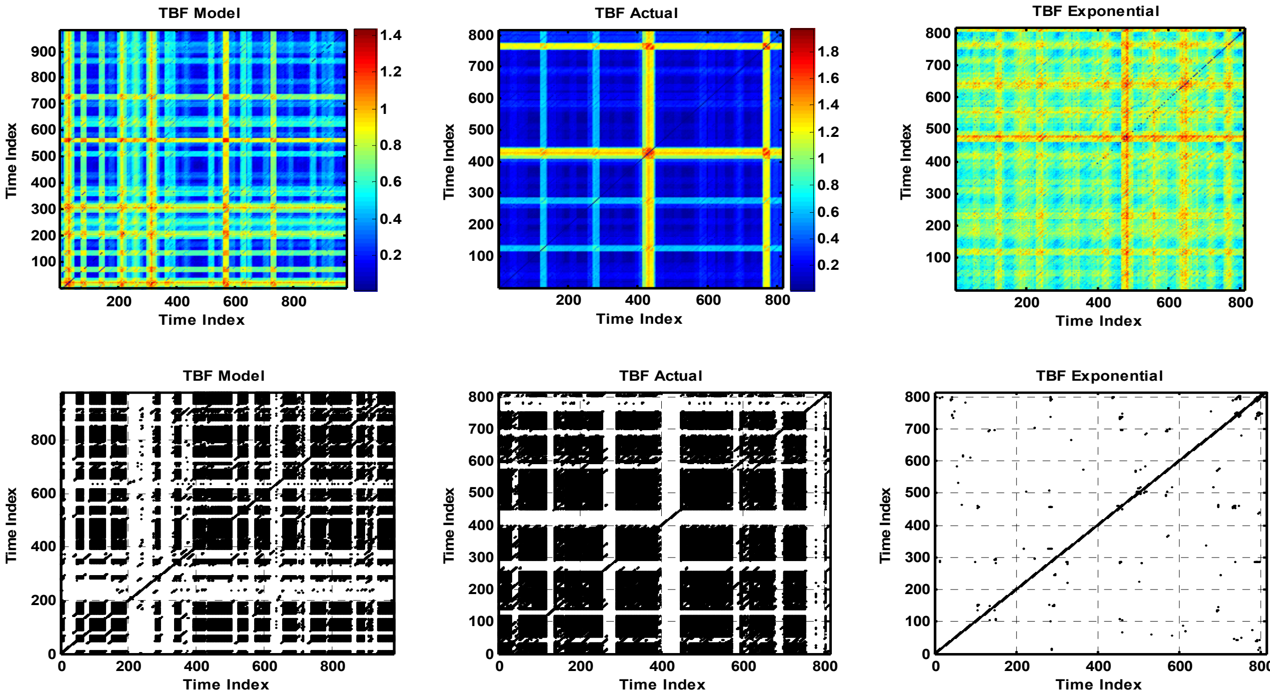

Fig. 8 *Comparison of TBF Recurrence Plots for Model, Actual and Exponential*

shows complete noise. The more blue (dark shade) and more yellow shade indicate the underlying non-stationarities in the signal.

Clearly, n-SDE model captures the certain intriguing and visually appealing patterns underlying the measured throughput data. The color map captures recurrence points identified at different neighborhood sizes. It may be noted that the patterns along vertical segments between two consecutive marked time indices are similar and nearly shifted versions of each other. Thus it is evident that recurrence patterns from the n-SDE model more closely capture the dynamics from actual data compared to a conventional exponential distribution model. The following recurrence quantifiers were used as metrics to quantify these recurrence patterns: (1) Recurrence rate, which measures the density of points in the recurrence plots; (2) Determinism, which measures the predictability of the system and is expressed in terms of the number of lines in the recurrence plot which lengths exceeding a specified threshold of l_{min}; (3) Laminarity that captures the mixing rates of the system; (4) Trapping time, which provides a measure of how long the system remains in a specific state; (5) Linemax which quantifies the divergence rates of trajectories in the system; (6) Shannon entropy that captures the complexity of the deterministic structure; and (7) Trend that determines the rate at which the density of the recurrence plots fade from the diagonal line.

Table 3 and Table 4 compare the quantifiers (quantification of recurrence plots) for TTR and TBF. As stated in the foregoing, these metrics are based on the recurrence point density, diagonal lines, and vertical lines structures of the recurrence plots [14, 15]. Table 3 and Table 4 reveals that the recurrence quantifiers of the model are much closer to actual compared to those from an exponential model. These results provide strong evidence that the present n-SDE modeling approach is superior to the commonly used exponential and other parametric distributions to capture TBF and TTR processes. Further investigations are necessary to develop this approach for effective (faster and more accurate) fitting of the downtime distributions and their interrelationships.

TABLE 3. COMPARISON OF TBF RECURRENCE QUANTIFIERS FOR MODEL, ACTUAL AND EXPONENTIAL

Metric	TBF			TBF Error %	
	Actual	Model	Exp	Model	Exp
Recrate	39.94	24.70	0.04	38%	100%
Determinism	97.48	96.94	25.32	1%	74%
Laminarity	115.00	82.00	8.00	29%	90%
Entropy	5.55	4.89	1.84	12%	62%
Trend	0.04	0.02	0.01	50%	50%
Linemax	90.70	91.25	0.00	-1%	100%
Trap. time	30.72	25.73	NaN	16%	>>100%

TABLE 4. COMPARISON OF TTR RECURRENCE QUANTIFIERS FOR MODEL, ACTUAL AND EXPONENTIAL

Metric	TTR			TTR Error %	
	Actual	Model	Exp	Model	Exp
Recrate	43.24	21.78	0.13	50%	99%
Determinism	97.84	97.90	51.31	0%	48%
Laminarity	115.00	102.00	30.00	11%	71%
Entropy	5.71	4.65	2.38	19%	49%
Trend	0.04	0.04	0.01	0%	75%
Linemax	92.08	95.32	0.00	-4%	100%
Trap. time	33.01	29.10	NaN	12%	>>100%

IV. CONCLUSIONS

The present work implemented analytical nonlinear stochastic differential equation (n-SDE) models to capture the dynamics of automotive manufacturing systems. Sigmoid function theory has been used to model downtime as the interplay between a machine degradation and restoration efforts. The n-SDE modeling approach was experimented on an 18 station assembly line segment in Matlab's Simulink© environment. The results were compared with those from a real-world production line observed during approximately one-year long period. The results show that the n-SDE model is significantly better at capturing the distribution of (marginal probability) of TBF and TTR compared to commonly used exponential distribution models. The model is also able to capture the salient trends in the assembly line dynamics, including the relative throughput losses due to blocking, starving, and machine breakdown. An extensive set of metrics were used to compare the statistical and nonlinear dynamical behaviors gathered from the models versus actual assembly line data. The model was found to capture the recurrence and other nonlinear behaviors of the assembly line dynamics better than conventional exponential distribution based models.

Our ongoing investigations will consider additional nuances of degradation dynamics (e.g., various structures for different modes of failure) and their implications on computational complexity and accuracy of simulations relative to the actual observations. We will also study the use of alternative sigmoid functional forms and the effects of linearization of the model on the stability and computational efficiency.

V. ACKNOWLEDGEMENT

The support of the National Science Foundation (CMMI-0729552) and General Motors towards the application of the proposed approach for the relevant manufacturing system operations is greatly acknowledged.

REFERENCES

[1] K. K. B. Hon, "Performance and Evaluation of Manufacturing Systems," *CIRP Annuals,* vol. 54, p. 675, 2005.

[2] D. Armbruster, G. Radons and R. Neugebauer, *Dynamical Systems and Production Systems, Chapter I in Nonlinear Dynamics of Production Systems*. Berlin: Wiley-VCH, 2004.

[3] D. Armbruster, and C. Ringhofer, "Thermalized kinetic and uid models for re-entrant supply chains," *SIAM J. Multiscale Modeling and Simulation,* In print 2005.

[4] D. Armbruster, R. Chidambaram, G. Godding, K. Kempf, and I. Katzorke, "Modeling and analysis of decision flows in complex supply networks," in *Proceedings of POMS*, Sao Paulo, 2001, pp. 1106 -1114.

[5] D. Armbruster and E. S. Gel, "Bucket Brigades Revisited: Are they always effective?," *preprint,* 2003.

[6] D. Armbruster, D. Marthaler, and C. Ringhofer, "Kinetic and fluid model hierarchies for supply chains," *SIAM Multiscale Modeling and Simulation,* vol. 2(1), pp. 43-61, 2004.

[7] D. Armbruster, C. Ringhofer, and T.-J. Jo, "Continuous models for production flow," in *American Control Conference*, Boston, 2004, pp. 4589 - 4594.

[8] J. Westman, and F. Hanson, "Computational Method for Nonlinear Stochastic Optimal Control," in *Proceedings of the 1999 American Control Conference*, 1999, pp. 2798-2802.

[9] N. Duffie, and I. Falu, CIRP "Control-theoretic analysis of a closed-loop PPC system," *Annals - Manufacturing Technology,* vol. 51, pp. 379-382, 2002.

[10] H. Wiendahl, and J. Breithaupt, "Backlog-oriented automatic production control," *CIRP Annals - Manufacturing Technology,* vol. 50, pp. 331-334, 2001.

[11] H. Wiendahl, N. Roth, and E. Westkamper, "Logistical positioning in a turbulent environment," *CIRP Annals - Manufacturing Technology,* vol. 51, pp. 383-386, 2003.

[12] H. P. Wiendahl and H. Scheffczyk, "Simulation based analysis of complex production systems with methods of nonlinear dynamics," *CIRP Annals,* vol. 48, p. 357, 1999.

[13] H. Yang, S. T. S. Bukkapatnam, and L. Barajas, "Nonlinear hybrid modeling of assembly line dynamics," *International journal of production research (under review),* 2007.

[14] J.-P. Eckmann, S. O. Kamphorst, and D. Ruelle, "Recurrence plots of dynamical systems," *Europhys Lett,* vol. 4, pp. 973-977, 1987.

[15] N. Marwan, "Encounters With Neighbours - Current Developments Of Concepts Based On Recurrence Plots And Their Applications." vol. Ph.D: University of Potsdam, 2003.